

A prospective intra-individual comparison of [⁶⁸Ga]Ga-PSMA-11 PET/CT, [⁶⁸Ga]Ga-NODAGA^{ZOL} PET/CT, and [^{99m}Tc]Tc-MDP bone scintigraphy for radionuclide imaging of prostate cancer skeletal metastases

Ismaheel O. Lawal^{1,2}, Kgomotso M.G. Mokoala¹, Johncy Mahapane¹, Janke Kleyhans^{1,2}, Marian Meckel³, Mariza Vorster^{1,2}, Thomas Ebenhan^{1,2}, Frank Rösch³, Mike M. Sathekge^{1,2}

1. Department of Nuclear Medicine, University of Pretoria & Steve Biko Academic Hospital, Pretoria, South Africa
2. Nuclear Medicine Research Infrastructure (NuMeRI), Steve Biko Academic Hospital, Pretoria, South Africa
3. Department of Chemistry, Johannes Gutenberg University Mainz, Mainz, Germany

Correspondence to: Mike Sathekge, Department of Nuclear Medicine, University of Pretoria and Steve Biko Academic Hospital, Private Bag X169, Pretoria, 0001, South Africa. E-mail: mike.sathekge@up.ac.za.

16 Digits ORCID:

IO Lawal: 0000-0003-4273-040X

MM Sathekge: 0000-0002-2806-0625

ABSTRACT

Purpose: Prostate cancer (PCa) commonly metastasize to the bones. There are several radionuclide techniques for imaging PCa skeletal metastases. We aimed to compare the lesion detection rate of [⁶⁸Ga]Ga-PSMA-11 PET/CT, [⁶⁸Ga]Ga-NODAGA-Zoledronate ([⁶⁸Ga]Ga-NODAGA^{ZOL}) PET/CT, and [^{99m}Tc]Tc-MDP bone scan in the assessment of bone metastases in patients with advanced PCa.

Methods: We prospectively recruited two cohorts of patients (staging and re-staging cohorts) with advanced prostate cancer. The staging cohort were treatment-naïve PCa patients imaged with [⁶⁸Ga]Ga-PSMA-11 PET/CT, [⁶⁸Ga]Ga-NODAGA^{ZOL} PET/CT, and bone scan. Re-staging cohort were patients who were previously treated with PSMA-based radioligand therapy and were experiencing PSA progression. The re-staging cohort was imaged with [⁶⁸Ga]Ga-PSMA-11 PET/CT and [⁶⁸Ga]Ga-NODAGA^{ZOL} PET/CT. We performed a per-patient and per-lesion analysis of skeletal metastases in both cohorts and made a comparison between scan findings.

Results: Eighteen patients were included with a median age of 68 years (range=48 - 80) and a median Gleason score of 8. There were ten patients in the staging cohort with a median PSA of 119.26 ng/mL (range=4.63 – 18,948.00) and eight patients in the re-staging cohort with a median PSA of 48.56 ng/mL (range=6.51 - 3175.00). In the staging cohort, skeletal metastases detected by [⁶⁸Ga]Ga-PSMA-11 PET/CT, [⁶⁸Ga]Ga-NODAGA^{ZOL} PET/CT, and bone scan were 322, 288, and 261, respectively, p=0.578. In the re-staging cohort, [⁶⁸Ga]Ga-PSMA-11 PET/CT and [⁶⁸Ga]Ga-NODAGA^{ZOL} PET/CT detected 152 and 191 skeletal metastases, respectively, p=0.529. In two patients with negative [⁶⁸Ga]Ga-PSMA-11 PET/CT findings, [⁶⁸Ga]Ga-NODAGA^{ZOL} detected one skeletal metastasis in one patient and 12 skeletal metastases in the other.

Conclusion: In patients with advanced prostate cancer, [⁶⁸Ga]Ga-PSMA-11 PET/CT may detect more lesions than [⁶⁸Ga]Ga-NODAGA^{ZOL} PET/CT and [^{99m}Tc]Tc-MDP bone scan for the staging of skeletal metastases. In patients who experience PSA progression on PSMA-based radioligand therapy, [⁶⁸Ga]Ga-NODAGA PET/CT is a more suitable imaging modality for the detection of skeletal lesions not expressing PSMA. In the setting of re-staging, [⁶⁸Ga]Ga-NODAGA^{ZOL} PET/CT may detect more lesions than [⁶⁸Ga]Ga-PSMA-11 PET/CT.

Keywords: Prostate cancer, Skeletal metastasis, [⁶⁸Ga]Ga-PSMA-11, [⁶⁸Ga]Ga-NODAGA^{ZOL}, [^{99m}Tc]Tc-MDP, Bone scan

INTRODUCTION

Prostate cancer (PCa) has a high predilection for spread to the bones. Up to 62% of patients with metastatic prostate cancer have bone-only metastasis [1]. The presence of bone metastasis is predictive of a shorter time to treatment failure and shorter overall survival in patients with PCa [1]. Skeletal metastases of PCa present with associated skeletal-related events, including pathologic fractures, cord compression, bone pain, and hypercalcemia, with an attendant negative impact of patients' quality of life [2]. The importance of bone metastases in PCa has stimulated the efforts to evaluate bone-targeted therapy resulting in the report confirming survival advantage conferred by radium-223 dichloride ($^{223}\text{RaCl}_2$) in the management of patients with bone-predominant PCa [2,3].

Determination of the presence of skeletal metastasis is essential in the staging and re-staging of PCa to determine optimum therapy and for prognostication. [$^{99\text{m}}\text{Tc}$]Tc-MDP bone scintigraphy (bone scan) is the only recommended radionuclide imaging modality for the assessment of bone metastasis in PCa. The per-patient pooled sensitivity and specificity of bone scan imaging of skeletal metastasis of PCa from a recent meta-analysis, including 27 studies were 79% and 82%, respectively [4]. Prostate-specific membrane antigen (PSMA) labeled with different radionuclides for positron emission tomography (PET) and single-photon emission tomography (SPECT) has recently emerged as an accurate technique for imaging of PCa in different settings [5-7]. PSMA is over-expressed in metastatic prostate cancer, which makes radio-labeled ligands such as [^{68}Ga]Ga-PSMA targeting membrane-expressed PSMA an attractive targeted imaging technique in PCa management. Zoledronic acid, a bisphosphonate, is a disease-modifying drug commonly used in PCa management for their ability to reduce disease-associated morbidity [8]. Gallium-68 has been successfully complexed to bis(phosphonic acid) using different linkers, including DOTA and NODAGA, for PET/CT imaging of skeletal metastases [9-11]. Like [$^{99\text{m}}\text{Tc}$]Tc-MDP and [^{223}Ra]RaCl₂, [^{68}Ga]Ga-NODAGA^{ZOL} accumulates in the region of bone turnover surrounding the PCa metastatic deposit in the bone, providing an indirect assessment of bone metastasis. The use of [^{68}Ga]Ga-NODAGA^{ZOL} for imaging of prostate cancer metastases is attractive because of its theranostic ability since zoledronic acid has also been successfully complexed with therapeutic radionuclides such as Lutetium-177 (^{177}Lu) and Actinium-225 (^{225}Ac) and may be indicated for therapy of PCa bone metastases when [^{223}Ra]RaCl₂ is not available [9,12-14].

A few studies have reported intra-individual comparison of [^{68}Ga]Ga-PSMA-11 PET/CT and bone scan [15-17]. No data is available regarding the comparative diagnostic performance of [^{68}Ga]Ga-NODAGA^{ZOL} versus other commonly applied radionuclide agents for the assessment of skeletal metastases in patients with PCa. In this study, we aimed to prospectively perform an intra-individual comparison of [^{68}Ga]Ga-PSMA-11 PET/CT, [^{68}Ga]Ga-NODAGA^{ZOL}, and [$^{99\text{m}}\text{Tc}$]Tc-MDP bone scan in the evaluation of bone metastases in men imaged for staging and re-staging of advanced prostate cancer.

PATIENTS AND METHODS

Patients

We prospectively recruited two cohorts of patients with advanced prostate cancer. Cohort 1 (staging cohort) consisted of patients with newly diagnosed histologically confirmed adenocarcinoma of the prostate gland. This cohort of patients showed skeletal metastases on [^{99m}Tc]Tc-MDP bone scan which was acquired first. They patients then had further imaging with [⁶⁸Ga]Ga-PSMA-11 PET/CT and [⁶⁸Ga]Ga-NODAGA^{ZOL}. The PET imaging was obtained in no particular order. In this cohort, consecutive patients who were referred to the department of Nuclear Medicine at Steve Biko Academic hospital between June 2017 and December 2017 for initial staging of PCa with [^{99m}Tc]Tc-MDP bone scan were evaluated for inclusion. Patients were included if they were newly diagnosed with PCa and had no other malignancies co-existing with prostate cancer. Patients who had commenced any form of therapy before imaging were excluded. In the second cohort (re-staging cohort), we recruited consecutive patients with bone-only or bone-predominant metastatic PCa who were treated with PSMA-based radioligand therapy (PRLT) between January 2018 and July 2019 and had no or minimal residual PSMA-avid skeletal lesions with decreasing avidity in the presence of rising serum levels of prostate-specific antigen (PSA). For the purpose of this study, we defined bone-predominant metastatic PCa as PCa with extensive skeletal metastases (20 skeletal lesions or more/metastatic superscan pattern) and oligometastatic soft tissue disease (4 or less soft tissue metastases). Patients in the re-staging cohorts had imaging with [⁶⁸Ga]Ga-PSMA-11 PET/CT and [⁶⁸Ga]Ga-NODAGA^{ZOL} to assess for residual prostate cancer skeletal metastases. In the re-staging cohort, imaging studies were done eight weeks after the last cycle of PRLT. In all patients, we obtained serum PSA within two weeks of the first imaging study. The Gleason score at histological diagnosis was retrieved from patients' records and recorded. All patients gave written informed consent to participate in the study and for the anonymous publication of their data. The Research Ethics Committee of the Faculty of Health Sciences, University of Pretoria, approved the study (Reference number: 20/2017).

Synthesis of radiotracers

[⁶⁸Ga]Ga-NODAGA^{ZOL}: ⁶⁸Ga was eluted from an 1850 MBq loaded ⁶⁸Ge/⁶⁸Ga generator (iThemba LABS, Somerset West, South Africa) using eluate fractionation and via a Jelco 22G X 1" polymer catheter (Smiths Medical, Croydon, South Africa) to obtain a metal-free radio-gallium transfer. 1 ml of radiogallium was added to a kit vial containing 45 µg buffered NODAGA^{ZOL} at a pH of 3.5 to 4. The mixture was heated in a heating block at 90-95°C for 10 minutes. Post labeling, Instant thin-layer chromatography (ITLC) was performed to determine the radiochemical purity of the labeled product. A sample (5 µl) of [⁶⁸Ga]Ga-NODAGA^{ZOL} was spotted on ITLC strip (MerckMillipore ITLC aluminum sheet with silica gel 60 Å, F254) and developed in a mobile phase solution (Acetyl Acetone + Acetonitrile + (0.6M) HCL). The developed ITLC strip (radioactivity) was counted and recorded on radio-chromatogram ($R_f = 0.0 - 0.2$ {⁶⁸Ga-NODAGA^{ZOL} (> 95%)}, $R_f = 0.8 - 1.0$ {free ⁶⁸Ga/ ⁶⁸Ga-colloids (<5%)}).

[⁶⁸Ga]Ga-PSMA-11: [⁶⁸Ga]Ga-PSMA-11 was synthesized in-house, as previously reported [18]. Briefly, 1 ml of the eluted [⁶⁸Ga]GaCl₃ was added to the kit vial containing PSMA-11. The

solution was incubated at room temperature for 15 minutes with gentle vortexing. 1.5 mL of 2.5 M sodium acetate trihydrate and 3 mL of normal saline was added to the solution to obtain a physiologic pH.

[^{99m}Tc]Tc-MDP: [^{99m}Tc]Tc-MDP was prepared according to published guidelines [19]. Briefly, freshly eluted sodium pertechnetate from a Molybdenum-99/Technetium-99 generator (NTP, Pelindaba, South Africa) was added to a vial containing sterile non-pyrogen lyophilized MDP at room temperature. 740 to 1110 MBq [^{99m}Tc]Tc-MDP was withdrawn from the solution for individual patient injection.

Image acquisition

No special patient preparation was obtained. PET/CT Imaging was commenced at 60 minutes post intravenous injection of [⁶⁸Ga]Ga-PSMA-11 and [⁶⁸Ga]Ga-NODAGA^{ZOL} on a hybrid Biograph 40 Truepoint PET/CT scanner (Siemens Medical Solution, IL, USA). Imaging parameters were similar for both [⁶⁸Ga]Ga-PSMA-11 and [⁶⁸Ga]Ga-NODAGA^{ZOL} PET/CT imaging, and image acquisition was from vertex to mid-thigh. The detailed imaging parameters are as we have previously reported [20,21].

Bone scintigraphy was acquired on an Infinia Hawkeye SPECT/CT camera (GE, WI, USA) or any one of two ECAM dual-headed SPECT cameras (Siemens Medical Solution, IL, USA). We performed imaging as per published guidelines [19]. Delayed whole-body imaging was performed two to four hours post tracer injection. This was followed by spot views of the chest (right anterior oblique, left anterior oblique, right posterior oblique, and left posterior oblique) and skull (right and left laterals). SPECT imaging of the thoracolumbar spine and pelvis was obtained after the spot views.

Image interpretation

Two experienced nuclear physicians performed image interpretation independently. Areas of disagreement were resolved by consensus. [⁶⁸Ga]Ga-PSMA-11 and [⁶⁸Ga]Ga-NODAGA^{ZOL} PET/CT image interpretation were done on a dedicated PET/CT workstation equipped with a syngo-via software. Areas of increased skeletal tracer uptake above background activity not due to physiologic processes were interpreted as sites of skeletal metastases. Bone changes seen on CT without corresponding increase tracer uptake on PET images were not considered as metastases. Even if these sites of non-tracer uptake were due to metastases, we disregarded them so that only PET data were used for image analysis in order to achieve a somewhat fair comparison between PET/CT imaging with [⁶⁸Ga]Ga-PSMA-11 PET and [⁶⁸Ga]Ga-NODAGA^{ZOL} versus bone scan that did not include CT imaging. In a per-patient analysis, we determined the ability of each of the tests to detect the presence of metastasis in an individual patient. We performed per-lesion analysis by counting the number of skeletal metastases each test detected in the individual patient. We counted individual focal skeletal lesions consistent with bone metastasis. When there was diffuse involvement of an entire bone such as seen in superscan pattern, we counted individual bone as a single lesion. We identified one lesion in each patient with the most intense tracer avidity of the PET scans and determined their maximum standard uptake value (SUVmax).

Bone scan image interpretation was done on a Xeleris workstation (GE Healthcare, WI, USA) or Syngo.via workstation (Siemens Medical Solution, IL, USA). Areas of increased tracer uptake in a manner typical of skeletal metastases were counted and recorded.

Statistical analysis

We performed a descriptive statistical analysis of the baseline clinical and disease characteristics of the patients. We expressed normally distributed variables as mean \pm standard deviation and skewed variables as median (range). We compared lesion detectability between the imaging tests using the Kruskal Wallis test. We compared SUVmax obtained on [⁶⁸Ga]Ga-PSMA-11 PET/CT versus SUVmax obtained on [⁶⁸Ga]Ga-NODAGA^{ZOL} using Paired-Samples T-test. We set statistical significance at a p-value of <0.05.

RESULTS

In total, we recruited 18 men with metastatic PCa with a median age of 68 years (range=48 - 80). There were ten patients in the staging cohort with a median PSA of 119.26 ng/mL (range=4.63 – 18,948.00) and a median Gleason score of 8 (range=6 - 9). Bone scan was the first imaging scan in all patients in the staging cohort. [⁶⁸Ga]Ga-PSMA-11 PET/CT was the second imaging study in six patients, while [⁶⁸Ga]Ga-NODAGA^{ZOL} PET/CT was the second imaging test in four patients. The median duration of the study tests (i.e., between bone scan as the first test and the last test, which could be either [⁶⁸Ga]Ga-PSMA-11 PET/CT or [⁶⁸Ga]Ga-NODAGA^{ZOL} PET/CT) was 23 days (range=17 - 31). There were eight patients included in the re-staging cohort with a median PSA of 48.56 ng/mL (range=6.51 - 3175.00) and a median Gleason score of 8 (range = 6 - 9). In 5 patients, [⁶⁸Ga]Ga-PSMA-11 PET/CT was the first imaging test obtained while [⁶⁸Ga]Ga-NODAGA^{ZOL} PET/CT was the first imaging test in three patients. The median interval between the two test scans in the re-staging cohort was eight days (range = 1 - 13). In all 18 patients, there was no significant difference in the activities of [⁶⁸Ga]Ga-PSMA-11 and [⁶⁸Ga]Ga-NODADA^{ZOL} administered to patients for imaging (147.32 versus 139.97 MBq, respectively – p>0.05). Table 1 shows a summary of the baseline clinical and disease characteristics of the patients included in this study.

Table 1: Baseline clinical and disease characteristics of the patients

S/N	Age (years)	Gleason score	PSA (ng/mL)	Indication for imaging
1	63	4+5	25.34	Staging
2	74	4+4	87.22	Staging
3	77	4+4	151.30	Staging
4	71	3+5	4.63	Staging
5	61	4+4	18,948.00	Staging
6	65	4+5	14.34	Staging
7	68	4+5	25.00	Staging
8	69	3+3	1436.00	Staging
9	48	4+5	280.58	Staging
10	79	4+4	179.37	Staging
11	70	4+4	1800.00	Re-staging
12	62	4+4	303.91	Re-staging
13	63	3+3	26.00	Re-staging
14	68	3+4	11.44	Re-staging
15	55	4+5	48.56	Re-staging
16	55	4+3	7.72	Re-staging
17	80	4+4	6.51	Re-staging
18	69	4+5	3175.00	Re-staging

Imaging findings: Staging cohort

[⁶⁸Ga]Ga-PSMA-11, [⁶⁸Ga]Ga-NODADA^{ZOL}, and bone scan had similar performance in per-patient analysis, with each imaging study detecting at least a site of skeletal metastasis. In a per-lesion analysis, [⁶⁸Ga]Ga-PSMA-11 PET/CT detected the most skeletal metastases in 5/10 patients, [⁶⁸Ga]Ga-NODAGA^{ZOL} detected the most skeletal metastases in 2/10 patients, bone scan detected the most skeletal metastases in 1/10 patient, and both [⁶⁸Ga]Ga-PSMA-11 PET/CT and bone scan detected an equal number of skeletal metastases in 1/10 patient and all three scans

detected an equal number of skeletal metastases in 1/10 patient (figure 1). Overall, [⁶⁸Ga]Ga-PSMA-11 PET/CT detected the most lesions in all patient (n=322 skeletal metastases, range=6-69) compared with 288 skeletal metastases for [⁶⁸Ga]Ga-NODAGA^{ZOL} PET/CT (range=5-72) and 261 skeletal metastases for bone scan (range=1-69), p=0.578. The most intensely-avid site of skeletal metastases was similar for both [⁶⁸Ga]Ga-PSMA-11 PET/CT and [⁶⁸Ga]Ga-NODAGA^{ZOL} in all patients with a mean SUVmax of 19.12 ± 8.37 versus 13.53 ± 8.92, p=0.165, respectively. In 8 of 10 patients, there were associated lymph node metastases detected on [⁶⁸Ga]Ga-PSMA-11 PET/CT. Figure 2 shows images of treatment-naïve patients with widespread skeletal metastases of prostate cancer.

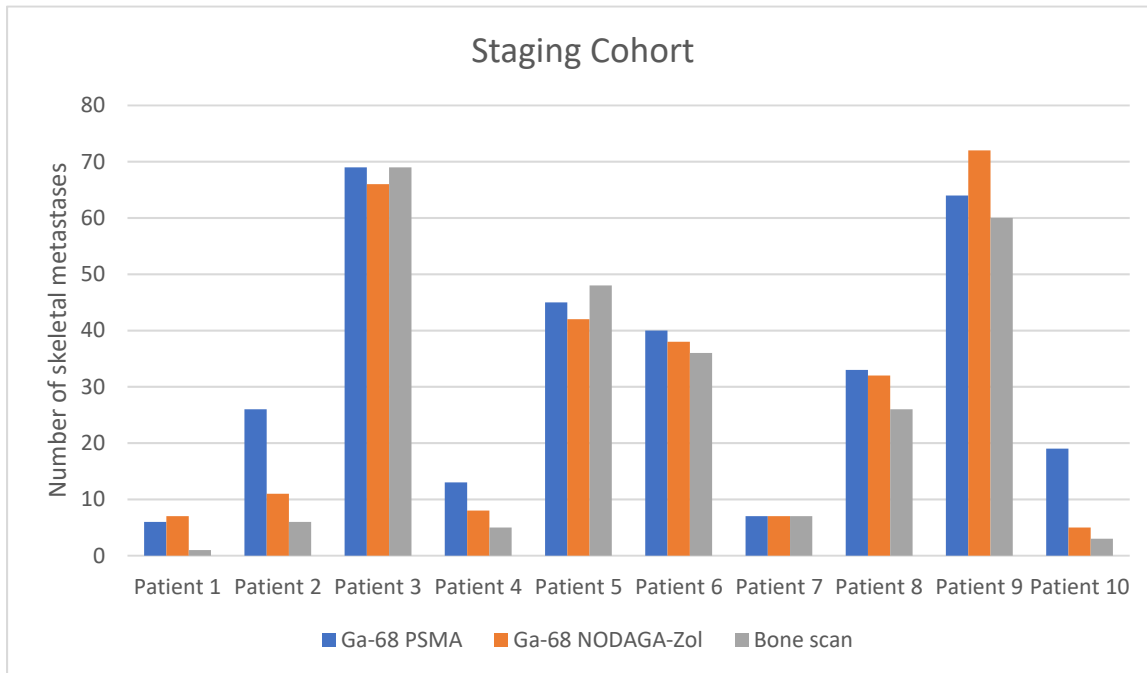


Figure 1: Chart showing the relative detection rates of [⁶⁸Ga]Ga-PSMA-11 PET/CT, [⁶⁸Ga]Ga-NODAGA^{ZOL}, and [^{99m}Tc]Tc-MDP bone scan in individual patients in the staging cohort.

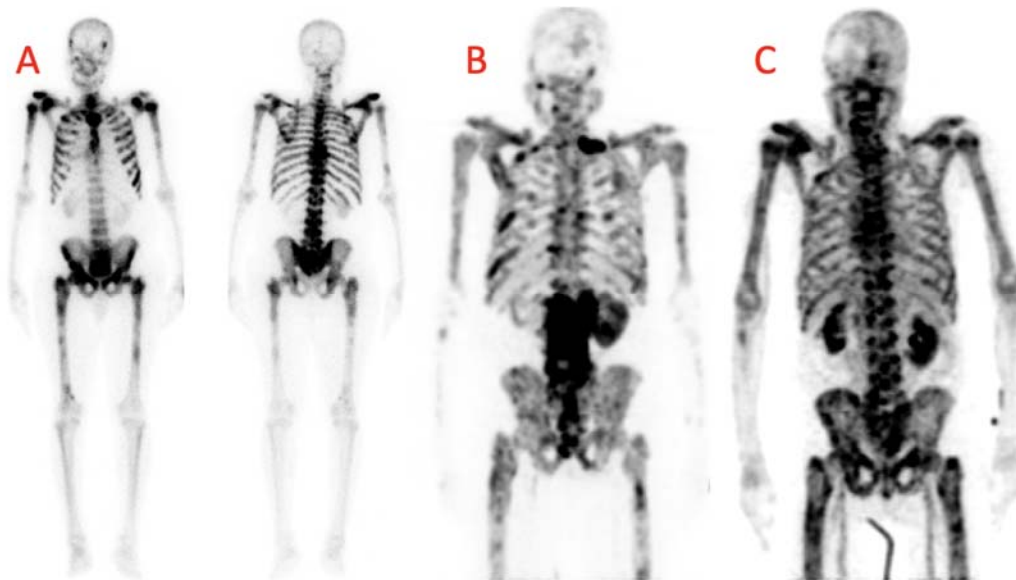


Figure 2: A 77-year-old man with newly-diagnosed prostate cancer, Gleason score of 4+4 and PSA of 151.3ng/mL. Anterior and posterior whole-body bone scan (A) and MIP images of $[^{68}\text{Ga}]\text{Ga-PSMA-11}$ PET/CT (B) and $[^{68}\text{Ga}]\text{Ga-NODAGA}^{\text{ZOL}}$ PET/CT (C) show widespread skeletal metastases with comparable lesion detectability between scans.

Imaging findings: Re-staging

$[^{68}\text{Ga}]\text{Ga-NODAGA}^{\text{ZOL}}$ PET/CT detected skeletal metastases in 8/8 patients, while $[^{68}\text{Ga}]\text{Ga-PSMA-11}$ PET/CT detected skeletal metastases in 6/8 patients (figure 3). In the two patients in whom $[^{68}\text{Ga}]\text{Ga-PSMA-11}$ PET/CT failed to detect any site skeletal metastasis, $[^{68}\text{Ga}]\text{Ga-NODAGA}^{\text{ZOL}}$ PET/CT detected 12 sites of skeletal metastases in one of them and one site of skeletal metastasis in the other (figure 4). In a per-lesion analysis, $[^{68}\text{Ga}]\text{Ga-NODAGA}^{\text{ZOL}}$ PET/CT detected more skeletal metastases than $[^{68}\text{Ga}]\text{Ga-PSMA-11}$ PET/CT in 6/8 patients while both scans detected an equal number of skeletal metastases in 2/8 patients. There was no patient in this cohort in whom $[^{68}\text{Ga}]\text{Ga-PSMA-11}$ PET/CT detected more skeletal metastases than $[^{68}\text{Ga}]\text{Ga-NODAGA}^{\text{ZOL}}$. Overall, $[^{68}\text{Ga}]\text{Ga-NODAGA}^{\text{ZOL}}$ PET/CT detected more lesions ($n=191$, range=1-76) compared with $[^{68}\text{Ga}]\text{Ga-PSMA-11}$ PET/CT ($n=152$, range=0-64), $p=0.529$. Similar lesions demonstrate the highest tracer avidity for both PET scans in all patients in this cohort as well, with a mean SUVmax of 20.57 ± 13.25 for $[^{68}\text{Ga}]\text{Ga-NODAGA}^{\text{ZOL}}$ PET/CT and 6.81 ± 3.76 for $[^{68}\text{Ga}]\text{Ga-PSMA-11}$ PET/CT, $p=0.035$. Figure 5 shows the images of a patient where $[^{68}\text{Ga}]\text{Ga-NODAGA}^{\text{ZOL}}$ PET/CT detected more skeletal metastases compared with $[^{68}\text{Ga}]\text{Ga-PSMA-11}$ PET/CT.

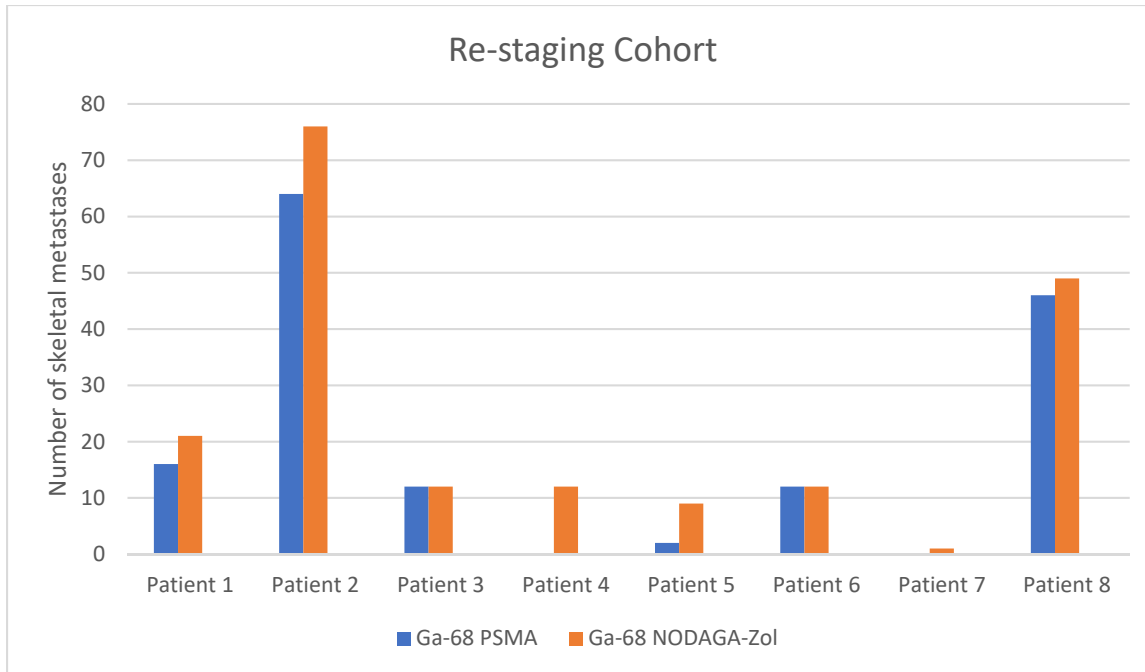


Figure 3: Chart showing the relative detection rates of $[^{68}\text{Ga}]\text{Ga-PSMA-11}$ PET/CT and $[^{68}\text{Ga}]\text{Ga-NODAGA}^{\text{ZOL}}$ in individual patients in the re-staging cohort. Two patients, patients 4 and 7, had negative findings on $[^{68}\text{Ga}]\text{Ga-PSMA-11}$ PET/CT.

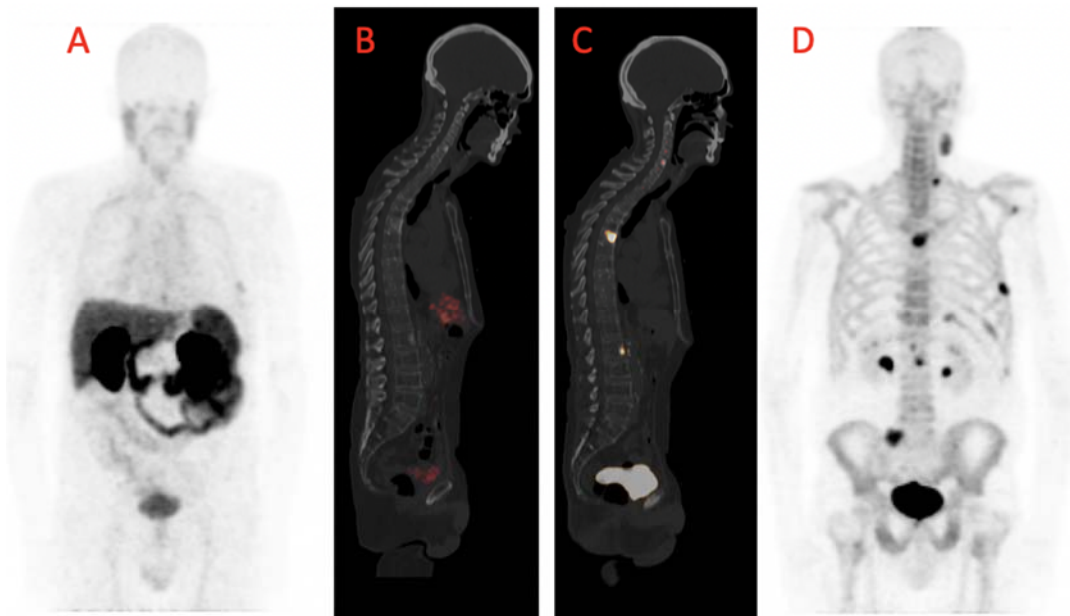


Figure 4: A 68-year-old male with hormone-resistant prostate cancer, Gleason score of 3+4, and a serum PSA of 11.44 ng/mL at the time of imaging. His treatment history includes radical prostatectomy, androgen deprivation therapy, radiotherapy for bone pain palliation, and four cycles of $[^{225}\text{Ac}]\text{-PSMA-617}$. MIP (A) and sagittal fused PET/CT (B) images of $[^{68}\text{Ga}]\text{-PSMA-11}$ PET/CT showed no lesion with avidity for the tracer significantly above background activity. In contrast, fused sagittal PET/CT (C) and MIP images (D) of the $[^{68}\text{Ga}]\text{Ga-NODAGA}^{\text{ZOL}}$ PET/CT show multiple sites of skeletal metastases.

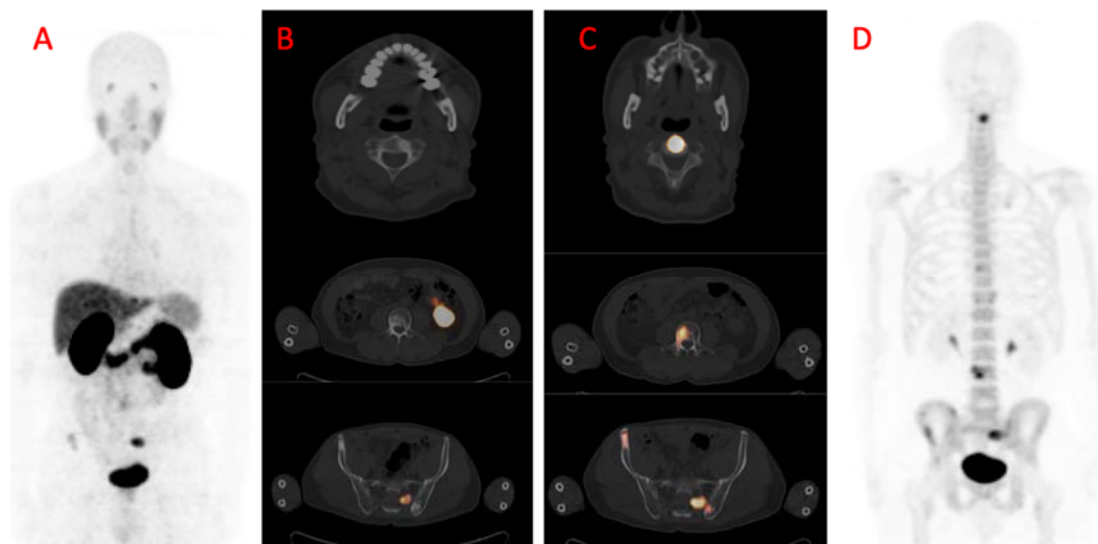


Figure 5: A 55-year-old male with metastatic prostate carcinoma, Gleason score of 4+5, PSA of 48.58 ng/mL. His prior treatment included androgen deprivation therapy and six cycles of [¹⁷⁷Lu]Lu-PSMA-617 therapy, followed by six cycles of [²²⁵Ac]Ac-PSMA-617 therapy. MIP image (A) and multiple fused axial PET/CT sections (B) of [⁶⁸Ga]Ga-PSMA-11 PET/CT show minimal skeletal metastases. Conversely, multiple fused axial PET/CT images (C) and MIP image (D) of [⁶⁸Ga]Ga-NODAGA^{ZOL} PET/CT show more extensive skeletal metastases.

DISCUSSION

In this prospective study, we evaluated the comparative detection rates of three radionuclide imaging tests for skeletal metastases in two cohorts of patients with advanced PCa. In the staging cohort and at an individual patient level, all three imaging tests had similar diagnostic performance detecting at least one site of skeletal metastases in all the patients in this cohort. At per-lesion level, [⁶⁸Ga]Ga-PSMA-11 PET/CT detected more lesions than [⁶⁸Ga]Ga-NODAGA^{ZOL} PET/CT, which in turn detected more lesions than bone scan. These differences in lesion detection rates did not, however, reach a statistical significance.

The lesion with the highest intensity for tracer uptake was similar between [⁶⁸Ga]Ga-PSMA-11 PET/CT and [⁶⁸Ga]Ga-NODAGA^{ZOL} PET/CT for patients without a significant difference in the SUVmax in each patient between the two PET scans.

Contrarily, in the re-staging cohort, which included patients we previously treated with targeted alpha therapy with [²²⁵Ac]Ac-PSMA-617, [⁶⁸Ga]Ga-NODAGA^{ZOL} PET/CT detected more skeletal lesions than [⁶⁸Ga]Ga-PSMA-11 PET/CT and detected skeletal metastases in two patients in whom [⁶⁸Ga]Ga-PSMA-11 PET/CT was falsely negative. These findings in the staging cohort, on a per-patient analysis, gives [⁶⁸Ga]Ga-PSMA-11 PET/CT, [⁶⁸Ga]Ga-NODAGA^{ZOL} PET/CT and bone scan similar sensitivity for the detection of skeletal metastases in patients with advanced prostate cancer. In the re-staging, in the setting of post PRLT, [⁶⁸Ga]Ga-NODAGA PET/CT has a higher sensitivity at the level of individual patient analysis compared with [⁶⁸Ga]Ga-PSMA-11 PET/CT.

The skeleton is a common site of distant metastases in PCa [1]. Accurate assessment of the skeleton for metastases is, therefore, germane, for the accurate staging of PCa. CT and bone scan are still recommended as the conventional imaging tests for PCa staging before definitive therapy with radical prostatectomy or radiotherapy [22,23]. Due to the limited sensitivity of combined CT and bone scan for the detection of skeletal metastases, many nuclear medicine techniques have been evaluated for skeletal metastases assessment [24,25]. PSMA expressed on PCa cells has become an attractive molecular target for imaging and therapy of advanced prostate cancer. The expression of PSMA on the cancer cells is an excellent opportunity to target the cancer directly for imaging and therapy. Many successes have been reported for PSMA-based imaging for the staging of advanced PCa, including its superior lesion detectability and its impact on treatment options [16,26]. In a recent multicenter randomized trial, [⁶⁸Ga]Ga-PSMA-11 PET/CT had a 27% greater accuracy compared with a combined bone scan and CT for initial staging of advanced prostate cancer [27]. Also, [⁶⁸Ga]Ga-PSMA-11 PET/CT was associated with less equivocal imaging findings, impacted more on management, and less radiation exposure than conventional imaging with combined CT and bone scan [27]. The ability of [⁶⁸Ga]Ga-PSMA-11 PET/CT to detect soft tissue metastases makes it a preferable one-stop shop imaging technique for PCa staging. In this study, 8 of 10 patients showed lymph node metastases in addition to skeletal metastases. In the staging cohort in our study, [⁶⁸Ga]Ga-PSMA-11 PET/CT detected more lesions compared with [⁶⁸Ga]Ga-NODAGA^{ZOL} and bone scan. The failure for the higher sensitivity of [⁶⁸Ga]Ga-PSMA-11 PET/CT to reach a statistical significance in our study may be related to our limited sample size. Bone scan continues to be an important modality in the initial staging of PCa. We think its importance may remain even with the appearance of more accurate imaging modalities for the assessment of skeletal metastases of PCa owing to its wider availability and lower cost.

We found a contrasting comparative performance for [⁶⁸Ga]Ga-PSMA-11 PET/CT versus [⁶⁸Ga]Ga-NODAGA^{ZOL} in the re-staging setting compared with the staging setting. In the re-staging cohort, [⁶⁸Ga]Ga-NODAGA^{ZOL} PET/CT performed better than [⁶⁸Ga]Ga-PSMA-11 PET/CT in the detection of skeletal metastases. The patients we recruited in this re-staging cohort had a rising serum PSA while on [²²⁵Ac]Ac-PSMA-617 therapy despite negative or improving imaging findings on [⁶⁸Ga]Ga-PSMA-11 PET/CT. These patients had bone-only or bone-predominant metastases of PCa, and we suspected down-regulation of PSMA expression in response to therapy pressure. Detection of more lesions on [⁶⁸Ga]Ga-NODAGA^{ZOL} PET/CT, including detection of skeletal lesions in patients in whom [⁶⁸Ga]Ga-PSMA-11 PET/CT imaging was negative, confirmed our suspicion. While PSMA is overexpressed in metastatic PCa and more so in the hormone-refractory stage of the disease, its expression is highly heterogeneous and dynamic [28]. Its expression is lower in early-stage organ-confirmed disease, increased in the metastatic phase, and may increase further in the hormone-refractory setting [29,30]. PCa may down-regulate this target in the very late stage of the disease [31]. This heterogeneity and dynamism of PSMA expression by PCa is the reason for baseline [⁶⁸Ga]Ga-PSMA-11 PET/CT to demonstrate tracer avidity in all lesions and, in recent times, for the call for additional ¹⁸F-FDG PET/CT imaging to evaluate for metastatic lesions not expressing PSMA [32]. In our cohort, we selected [⁶⁸Ga]Ga-NODAGA^{ZOL} PET/CT as the additional imaging to evaluate for lesions not expressing PSMA for two reasons. Firstly, these patients had bone-only or bone-predominant

metastatic PCa, and secondly and based on the first reason, we were considering these patients for targeted alpha therapy with ^{225}Ac -labeled Zoledronate.

Like ^{223}Ra $[\text{RaCl}_2]$, Zoledronate accumulates in the region of osteoblastic response mounted by the bone tissue around metastatic deposit in the marrow. Zoledronate inhibits osteoclasts activity, reducing skeletal-related events in skeletal metastases of malignant disease [8]. Zoledronate has been successfully labeled with Lutetium-177 (^{177}Lu) and ^{225}Ac for targeted beta and alpha therapies of skeletal metastases of prostate cancer, respectively [9,12-14]. PRLT with either ^{177}Lu Lu-PSMA-617 or ^{225}Ac Ac-PSMA-617 is currently applied as last-line agents in patients who have exhausted or are unfit for approved agents. When disease progression occurs following PRLT, treatment options are limited. ^{177}Lu or ^{225}Ac -labeled Zoledronate may be explored for salvage therapy. In this case, imaging is necessary to predict Zoledronate accumulation in skeletal lesions. We demonstrated significantly more intense ^{68}Ga Ga-NODAGA^{ZOL} uptake in skeletal metastases, which makes Zoledronate-based theranostics a viable treatment option. Pfannkuchen and colleagues showed that ^{68}Ga Ga-NODAGA^{ZOL} labeled fast without the need for purification and had a higher target-to-background ratio compared with ^{68}Ga Ga-DOTA^{ZOL} [33]. This makes ^{68}Ga Ga-NODAGA^{ZOL} a promising theranostic companion for ^{177}Lu Lu-DOTA^{ZOL} [33].

A major limitation of our study is its small study population. Despite this limitation, we were able to show, for the first time, the relative performance of three different radionuclide imaging techniques for the detection of prostate cancer skeletal metastases in a prospectively recruited study. Our results may form the basis for the design of future studies and have the potential to guide the clinical application of radionuclide techniques in the evaluation of skeletal metastases of prostate cancer. In this study, we showed different performance of two PET tracers for the detection of skeletal metastases in two different settings. Patients in the staging group had three radionuclide imaging tests, while patients in the re-staging group had two imaging tests done for this study. The considerable radiation exposure imposed by these multiple radionuclide tests contributes to the limited patients recruited. Another limitation of our study is the lack of histological confirmation of skeletal metastases. Patients included in this study had advanced prostate cancer based on their high serum PSA, Gleason score, and treatment history. Based on these, there is already a high risk for skeletal metastases. Also, most patients had multiple skeletal metastases, and it would be unethical and unfeasible to biopsy all lesion to determine their true nature. Including patients with a high burden of skeletal metastases in the staging cohort, especially patients with diffuse skeletal metastases in the superscan pattern, presented another limitation. In order to compare lesion detection rates between imaging modalities in these patients with a superscan pattern, we resulted to counting individual involved bone as a single lesion. ^{68}Ga Ga-NODAGA^{ZOL} is not tumor-specific and may accumulate at the site of reparative changes in response to PRLT which was administered to patients in the re-staging cohort. This is unlikely in this case as these patients had a declining or absence tracer avidity in bone lesions on ^{68}Ga Ga-PSMA-11 PET/CT despite a rising serum PSA. They did not have new soft tissue metastases with or without PSMA expression. Even with this precaution, a false positive on ^{68}Ga Ga-NODAGA^{ZOL} PET/CT cannot be completely excluded without biopsy for histological confirmation of PSMA-negative skeletal metastases of PCa.

Correlative imaging with [¹⁸F]F-FDG PET/CT could be used as an alternative for disease confirmation. [¹⁸F]F-FDG PET/CT was, unfortunately, not done in these patients.

CONCLUSION

In patients with advanced prostate cancer, [⁶⁸Ga]Ga-PSMA-11 PET/CT detected more lesions compared with [⁶⁸Ga]Ga-NODAGA^{ZOL} PET/CT and [^{99m}Tc]Tc-MDP bone scan for the staging of skeletal metastases. Vice versa, in patients who experience PSA progression on PSMA-based radioligand therapy, [⁶⁸Ga]Ga-NODAGA^{ZOL} PET/CT is a more suitable imaging modality for the detection of skeletal lesions not expressing PSMA. In the setting of re-staging, [⁶⁸Ga]Ga-NODAGA^{ZOL} PET/CT may outperform [⁶⁸Ga]Ga-PSMA PET/CT in the quantification of skeletal metastases and may also be useful to guide the application of Zoledronate-based theranostics of prostate cancer.

COMPLIANCE WITH ETHICAL STANDARDS

Funding: No external funding was received in the conduct of this study.

Conflicts of interest: All authors declare that they have no conflict of interest.

Ethical approval: This study was performed in accordance with the ethical standard of our institutions and with the 1964 Helsinki Declaration and its later amendments or comparable ethical standards.

Consent to participate: All patients gave written informed consent to participate in the study.

Consent for publication: All patients provided informed consent to allow for the publication of their anonymized data collected during this study.

Availability of data and material: All data collected during the conduct of this study are included in this report.

References

1. James ND, Spears M, Clarke NW, Dearnaley DP, De Bono JS, Gale J, et al. Survival with newly diagnosed metastatic prostate cancer in the “docetaxel era”: Data from 917 patients in the control arm of the STAMPEDE trial (MRC PR08, CRUK/06/019). *Eur Urol.* 2015;67:1028-1038.
2. Brito AE, Etchebehere E. Radium-223 as an approved modality for treatment of bone metastases. *Semin Nucl Med.* 2020;50:177-192.
3. Parker C, Nilsson S, Heinrich D, Helle SI, O’Sullivan JM, Fosså SD, et al. Alpha emitter radium-223 and survival in metastatic prostate cancer. *N Engl J Med.* 2013;369:213-223.
4. Shen G, Deng H, Hu S, Jia Z. Comparison of choline-PET/CT, MRI, SPECT, and bone scintigraphy in patients with prostate cancer: a meta-analysis. *Skeletal Radiol.* 2014;43:1503-1513.

5. Lawal IO, Ankrah AO, Mokgoro NP, Vorster M, Maes A, Sathekge MM. Diagnostic sensitivity of Tc-99m HYNIC PSMA SPECT/CT in prostate carcinoma: A comparative analysis with Ga-68 PSMA PET/CT. *Prostate*. 2017;77:1205-1212.
6. Perera M, Papa N, Roberts M, Williams M, Udovicich C, Vela I, et al. Gallium-68 prostate-specific membrane antigen positron emission tomography in advanced prostate cancer—updated diagnostic utility, sensitivity, specificity, and distribution of prostate-specific membrane antigen-avid lesions: A systemic review and meta-analysis. *Eur Urol*. 2020;77:403-417.
7. Giesel FL, Will L, Lawal I, Lengana T, Kratochwil C, Vorster M, et al. Intraindividual comparison of ¹⁸F-PSMA-1007 and ¹⁸F-DCFPyL PET/CT in the prospective evaluation of patients with newly diagnosed prostate carcinoma: A pilot study. *J Nucl Med*. 2018;59:1076-1080.
8. Saad F, Gleason DM, Murray R, Tchekmedyian S, Venner P, Lacombe L, et al. Long-term efficacy of zoledronic acid for the prevention of skeletal complications in patients with metastatic hormone-refractory prostate cancer. *J Natl Cancer Inst*. 2004;96:879-882.
9. Pfannkuchen N, Meckel M, Bergmann R, Bachmann M, Bal C, Sathekge M, et al. Novel radiolabeled bisphosphonates for PET diagnosis and endoradiotherapy of bone metastases. *Pharmaceutical (Basel)*. 2017;10:45.
10. Khawar A, Eppard E, Roesch F, Ahmadzadehfar H, Kürpig S, Meisenheimer M, et al. Preliminary results of biodistribution and dosimetric analysis of [⁶⁸Ga]Ga-DOTA^{ZOL}: a new Zoledronate-based bisphosphonate for PET/CT diagnosis of bone disease. *Ann Nucl Med*. 2019;33:404-413.
11. Holub J, Meckel M, Kubíček V, Rösch F, Hermann P. Gallium(III) complexes of NOTA-bis(phosphonate) conjugates as PET radiotracers for bone imaging. *Contrast Media Mol Imaging*. 2015;10:122-134.
12. Bergmann R, Meckel M, Kubíček V, Pietzsch J, Steinbach J, Hermann P, et al. (177)Lu-labelled macrocyclic bisphosphonates for targeting bone metastasis in cancer treatment. *EJNMMI Res*. 2016;6:5.
13. Khawar A, Eppard E, Roesch F, Ahmadzadehfar H, Kürpig S, Meisenheimer M, et al. Biodistribution and post-therapy dosimetric analysis of [¹⁷⁷Lu]Lu-DOTA^{ZOL} in patients with osteoblastic metastases: first results. *EJNMMI Res*. 2019;9:102.
14. Pfannkuchen N, Bausbacher N, Pektor S, Miederer M, Rosch F. *In vivo* evaluation of [²²⁵Ac]Ac-DOTA^{ZOL} for α -therapy of bone metastases. *Curr Radiopharm*. 2018;11:223-230.
15. Thomas L, Balmus C, Ahmadzadehfar H, Essler M, Strunk H, Bundschuh RA. Assessment of bone metastases in patients with prostate cancer – a comparison between ^{99m}Tc-bone-scintigraphy and [⁶⁸Ga]Ga-PSMA PET/CT. *Pharmaceuticals*. 2017;10:68.
16. Lengana T, Lawal IO, Boshomane TG, Popoola GO, Mokoala KMG, et al. ⁶⁸Ga-PSMA PET/CT replacing bone scan in the initial staging of skeletal metastasis in prostate cancer: a fait accompli? *Clin Genitourin Cancer*. 2018;16:392-401.
17. Zacho HD, Nielsen JB, Haberkorn U, Stenholt L, Petersen LJ. ⁶⁸Ga-PSMA PET/CT for the detection of bone metastases in prostate cancer: a systematic review of published literature. *Clin Physiol Funct Imaging*. 2018;38:911-922.

18. Ebenhan T, Vorster M, Marjanovic-Painter B, Wagener J, Suthiram J, Modiselle M, et al. Development of a single vial kit solution for radiolabeling of ⁶⁸Ga-DKFZ-PSMA-11 and its performance in prostate cancer patients. *Molecules*. 2015;20:14860-14878.
19. Van den Wyngaet T, Strobel K, Kampen WU, Kuwert T, van der Gruggen W, Mohan HK, et al. The EANM practice guidelines for bone scintigraphy. *Eur J Nucl Med Mol Imaging*. 2016;43:1723-1738.
20. Lengana T, van de Wiele C, Lawal I, Maes A, Ebenhan T, Boshomane T, et al. ⁶⁸Ga-PSMA-HBED-CC PET/CT imaging in Blacks versus White South African patients with prostate carcinoma presenting with a low volume, androgen-dependent biochemical recurrence: a prospective study. *Nucl Med Commun*. 2018;39:179-185.
21. Sathekge M, Lengana T, Maes A, Vorster M, Zeevaart JR, Lawal I, et al. ⁶⁸Ga-PSMA-11 PET/CT in primary staging of prostate carcinoma: preliminary results on differences between black and white South-Africans. *Eur J Nucl Med Mol Imaging*. 2018;45:226-234.
22. Mottet N, van den Bergh RCN, Briers E, Cornford P, De Santis M, Fanti S, et al. EAU-EANM-ESTRO-ESUR-SIOG guidelines on prostate cancer. Available from <https://uroweb.org>. Accessed on 29 March 2020.
23. Donohoe KJ, Cohen EJ, Giammarile F, Grady E, Greenspan BS, Henkin RE, et al. Appropriate use criteria for bone scintigraphy in prostate and breast cancer: summary and excerpts. *J Nucl Med*. 2017;58:14N-17N.
24. Esen T, Kihç M, Seymen H, Acar Ö, Demirkol MO. Can Ga-68 PSMA PET/CT replace conventional imaging modalities for primary lymph node and bone staging of prostate cancer? *Eur Urol Focus*. 2020;6:218-220.
25. Turpin A, Girard E, Baillet C, Pasquier D, Olivier J, Villers A, et al. Imaging for metastasis in prostate cancer: A review of the literature. *Front Oncol*. 2020;10:55.
26. Roach PJ, Francis R, Emmet L, Hsiao E, Kneebone A, Hruby G, et al. The impact of ⁶⁸Ga-PSMA PET/CT on management intent in prostate cancer: Results of an Australian prospective multicenter study. *J Nucl Med*. 2018;59:82-88.
27. Hofman MS, Lawrentschuk N, Francis R, Tang C, Vela I, Thomas P, et al. Prostate-specific membrane antigen PET-CT in patients with high-risk prostate cancer before curative-intent surgery or radiotherapy (proPSMA): a prospective, randomized, multi-centre study. *Lancet*. Epub ahead of print on March 22, 2020.
28. Paschalis A, Sheehan B, Riisnaes R, Rodrigues DN, Gurel B, Bertan C, et al. Prostate-specific membrane antigen heterogeneity and DNA repair defects in prostate cancer. *Eur Urol*. 2019;76:469-478.
29. Sweat SD, Pacelli A, Murphy GP, Bostwick DG. Prostate-specific membrane antigen expression is greatest in prostate adenocarcinoma and lymph node metastases. *Urology*. 1998;52:637-640.
30. Bostwick DG, Pacelli A, Blute M, et al. prostate specific membrane antigen expression in prostatic intraepithelial neoplasia and adenocarcinoma: a study of 184 cases. *Cancer*. 1998;82:2256-2261.
31. Emmett L, Crumbaker M, Ho B, Willowson K, Eu P, Ratnayake L, et al. Results of a prospective phase 2 pilot trial of ¹⁷⁷Lu-PSMA-617 therapy for metastatic castration-resistant prostate cancer including imaging predictors of treatment response and patterns of progression. *Clin Genitourin Cancer*. 2019;17:15-22.

32. Hofman MS, Emmett L. Tumour heterogeneity and resistance to therapy in prostate cancer: A fundamental limitation to prostate-specific membrane antigen theranostics or a key strength. *Eur Urol.* 2019;76:479-481.
33. Pfannkuchen N, Bergmann R, Pietzsch J, Bachmann M, Roesch F. DOTA^{Zn} and NODAGA^{Zn} for theranostics of bone metastases. [abstract]. *J Nucl Med.* 2017;58(Suppl 1):324.